# Hydrological modeling to assess the link between water availability and vegetation growth

Ingrid Teich[1,2], César Luis García[1,2], Carolien Tote[3], Else Swinnen[3], Ana Planchuelo[1,2], Mónica Balzarini[1,4]

[1] *National Council of Scientific and Technological Research (CONICET), Argentina*
[2] *CREAN, Faculty of Agronomic Sciences, National University of Córdoba, Argentina*
[3] *Centre for Remote Sensing & Earth Obs. Processes (TAP), Flemish Inst. for Technol. Res. (VITO), Belgium.*
[4] *Applied Statistics, Faculty of Agronomic Sciences, National University of Córdoba, Argentina*

**Abstract**: In the face of climate change and for sustainable management of arid areas, it is crucial to understand the link between water availability and vegetation growth. This linkage is often investigated using time series of rainfall data and a vegetation index from satellite sensors (e.g. NDVI). However, rainfall alone is not sufficient to describe available water for vegetation, and other bio-geophysical factors should be taken into account. Hydrological modeling offers a powerful tool for this purpose. In this study, hydrological response units (HRU) delineated in a distributed hydrological model system (JAMS), were used to compute a complete water balance and to assess the vegetation response to climatic variability in a Mountain Basin (Córdoba, Argentina). Vegetation changes were analyzed through NDVI time series from SPOT-VEGETATION images over the 12 year period 1998-2009. Precipitation was always the least correlated variable to vegetation growth, except in less vegetated rocky areas. Synchrony of the vegetation growth with soil water saturation was found to be more direct (less delay), specially in grasslands. Our results show that hydrological modeling can aid in the study of vegetation response to climate variability, high lightening the importance of taking into account other factors that influence water availability besides precipitation.

**Keywords**: NDVI, distributed model, Hidrological Response Units

## Introduction

Water runs through very different systems, such as air, vegetation or soil, creating a complex web of interactions. Plant growth and productivity depend on available water (Jobbágy *et al.,* 2002). In parallel, and through this demand, plants exert a strong influence on many key hydrologic variables (Nosetto *et al.,* 2011). Given the current scenario of global change, increased population and food insecurity, studies towards an understanding of the role of water in the interface between the “geo-spheres” (litho, hydro, bio, and atmo-spheres) are crucial. Many studies have focused on ecosystem responses to climate variability (Walther *et al.* 2002). Others have contributed in disentangling the effects of land cover change on the water balance and the quantity and quality of water resources (Krause, 2002; Viglizzo *et al*. 2010). In this quest, remote sensed information has aided significantly as it offers the possibility to measure different environmental characteristics over wide areas and long time periods. Also hydrological modeling is becoming an essential tool to study associations between the water cycle and land cover changes.

The Normalized Difference Vegetation Index (NDVI) (Tucker, 1979), is one of the most extensively used remote-sensing based vegetation indices. NDVI data provide estimates of vegetation photosynthetic activity that can be related to primary productivity, leaf area, canopy coverage, and chlorophyll density, as well as to vegetation phenology. NDVI data is regarded as a reliable indicator for land cover conditions and variations over the years, being widely used for vegetation monitoring. For example, Seaquist *et al.* (2003) developed a NDVI based primary production model for grassland biomass; Birky (2001) developed a linear model relating NDVI to leaf biomass and specific gross primary productivity; Ludeke *et al.* (1996) used satellite NDVI for the validation of global vegetation phenology. Relating the NDVI to climatic variables has allowed to explore and predict the response of vegetation to environmental variability. In this context, NDVI was found to relate well with precipitation and to be highly sensitive to rainfall anomalies such as drought (Kogan, 2000; Li & Kafatos, 2000). However, this relationship is controlled by other factors such as land-cover type and climate conditions (Camberlin *et al.*, 2007). Therefore, considering additional information of the water cycle can significantly improve our knowledge and prediction capacity of productivity changes under different climatic scenarios.

Hydrological models are simplified, conceptual representations of a part of the hydrological cycle, primarily used for prediction and for understanding hydrologic processes. Distributed models, in contrast to aggregated ones, do not consider catchments as a unique unit but distribute the components of the water cycle into smaller modelling units. In the model J2000g (Krause and Hanisch, 2009), this units are Hydrological Response Units (HRUs), and are defined by many characteristics, such as topography, land-use, soil type and hydrogeology. The HRUs represent areas with a homogeneous hydrological response (Flügel, 1995). In each HRU, the hydrological cycle is modeled and each component is computed on every cycle. This information, which not only takes into account meteorological variables, but also land use and geological data, can be of great help to improve the correlation between climatic variability and productivity.

In this work we propose the use of variables obtained by a distributed hydrological model to examine temporal responses of remotely sensed NDVI environmental variability during a twelve year period (1998-2009). We test the hypothesis that actual evapotranspiration and water saturation will have higher correlations coefficients with NDVI than precipitation. We also compare these correlations between several land cover types in a semi-arid region of central Argentina.

## Methods

*Study area*

This study was performed in the San Antonio river Basin, located in the central portion of the Sierras Grandes of Córdoba, Argentina (1800–2400 m a.s.l., 31°34 S, 64°50 W), in central Argentina (Fig. 1). In the high plateau the mean temperature of the coldest and warmest months are 5.0 and 11.4 C, respectively, and there is no frost-free period. Mean annual precipitation is 818 mm, with most rainfall concentrated in the warmer months, between October and April. The area comprises different landscape units, including valley bottoms and ravines, plateaus with different degrees of dissection, rocky hilly uplands and steep escarpments. Most of these units (with the exception of plateaus with low dissection) are rough, with abundant rocky outcrops, steep slopes and high topographic variability at short distances (Cingolani *et al.*, 2004). Vegetation consists of a mosaic of tussock grasslands, grazing lawns, granite outcrops, *Polylepis australis* woodlands, and eroded areas with exposed rock surfaces (Cabido, 1985; Cingolani *et al.*, 2004). The basin has an area of 520 $km^2$ and the water sources are located at 2200 m asl. The main direction of the flow is west, ending in the San Roque Lake, one of the main water reservoirs of the province.

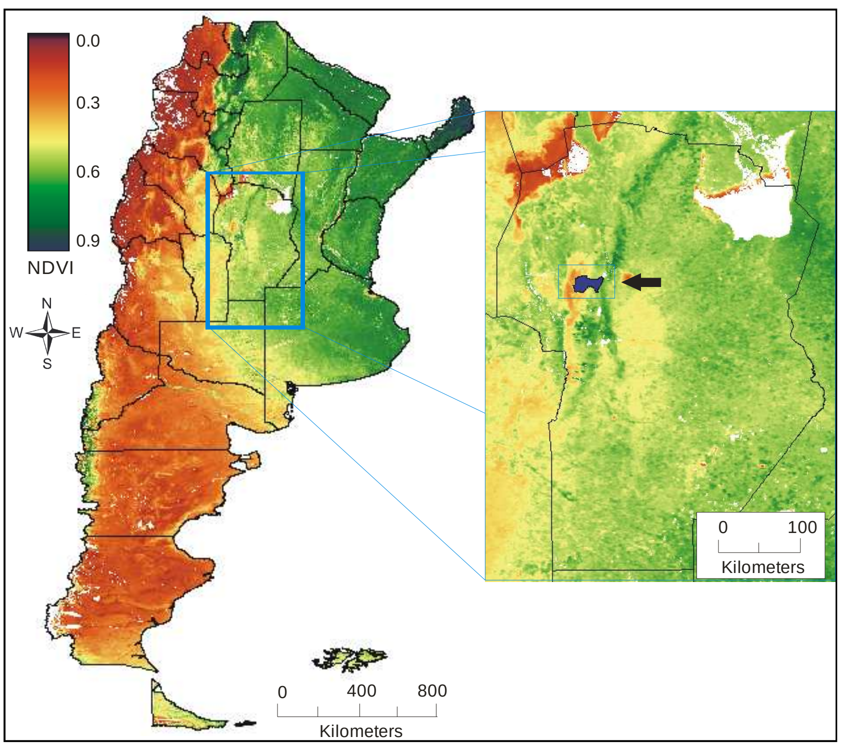


**Figure 1:** Map of Argentina showing the average NDVI for the studied period: April 1998 to December 2009, and zoom of the study area. The arrow indicate the location of the San Antonio River Basin.

*Vegetation growth*

NDVI time series from April 1998 till December 2009 were obtained from the VEGETATION sensor on board the SPOT satellite platforms. Such data are available free of charge at the Vlaamse Instelling voor Technologisch Onderzock (VITO) Image Processing centre (Mol, Belgium) (http://www.vgt.vito.be). The NDVI is based on the red (R) and near infra red (NIR) spectral bands of which the remote sensor registers the portion of the reflected radiation. Since green plants use red radiation for photosynthesis, their red reflectance is low compared to other types of land cover. The NIR reflectance is higher for vegetation than for bare soil, because of multiple scattering in the plants and plant cells. NDVI is calculated as:

$$NDVI = \frac{NIR - R}{NIR + R}$$

The magnitude of NDVI is related to the level of photosynthetic activity in the observed vegetation. Generally, higher positive values of NDVI indicate vigor and quantity of vegetation, whereas low values are usually associated with non-vegetated areas. This means that the evolution of vegetation growth can be observed using repeated NDVI measurements.

The 10-day SPOT-VEGETATION NDVI data at 1km ×1km spatial resolution used as input for this study were preprocessed to take into account radiometric calibration, atmospheric and geometric correction, as well as cloud removal. Daily images were combined into 10-day composites (S10) by selecting the maximum NDVI within the compositing period (1-10, 11-20 and 21-end of month), resulting in 36 dekads per year. Compositing into dekadal images reduces cloud contamination (Lewis *et al*., 1998), but is still sufficient to capture the evolution of vegetation growth over time. When considering the time domain, the NDVI time series still contains noise due to undetected clouds/haze, viewing geometry and local aerosols in the atmosphere. The temporal profiles were therefore further smoothed using the modified Swets-method (Swets *et al*., 1999) implemented in GLIMPSE Software (Global Image Processing Software, Eerens 2010). Smoothing was executed for a full year of data spanning an entire growing season and was done in two steps. First, suspicious low and high values were identified based on a number of parameters. Secondly, these values were replaced using polynomial interpolation.

*Hydrological modeling*

To model the basin water cycle components, we recently implemented the J2000g model (Krause and Hanisch, 2009) within the JAMS modeling framework system (Kralisch and Krause, 2006). This model can be categorized as a spatially distributed conceptual hydrological model with a low number of calibration parameters. J2000g requires few meteorological inputs (precipitation; minimum, average and maximum temperature and extraterrestrial solar radiation).The potential evapotranspiration (potET) was calculated according to Hargreaves-Samani method (Samani, 2000) which requires only temperature and extraterrestrial solar radiation calculations. The real evaporation (ET) is calculated with consideration of the current soil humidity. A correction function is applied under the assumption that below certain water content level, the real evaporation decreases proportionally to the potential evaporation until it becomes zero at the permanent wilting point. Snow accumulation and snowmelt are simulated with a day-degree approach followed by a soil moisture accounting module consisting of simple water storage with a capacity defined from the field capacity of the specific soil type within the respective modeling unit. Water stored in the soil water storage can only be taken out through evapotranspiration. Runoff is generated only when the soil water storage is at saturation and partitioned into direct runoff and percolation based on the slope of the modeling unit and the underlying hydrogeology. The percolation component is transferred to ground water storage and baseflow by a linear storage model. The total streamflow of a catchment results from the summation of the direct runoff and the baseflow components from each modeling unit.

The storage concept used in the J2000g considers the hydrological conditions inside the soil profile by two different storages. The first one is the middle pore storage (MPS) describing the water storage capacity of the middle sized pores (diameter 0.2–50 µm). In such pores water is held against gravity and can only be drained out by an active tension. The second storage called large pore storage (LPS) describes the water storage capacity of pores with diameter > 50 µm, which are not able to hold the water against gravity and are therefore considered as the source for vertical and horizontal flow. The storage capacity of the MPS and LPS is determined by the description of soil profiles together with the effective rooting depth of the land use class for each HRU.

*Correlations between NDVI and climatic variability*

Given that NDVI pixels of 1km×1km have a coarser spatial resolution than HRUs, we extracted data at NDVI spatial resolution (Fig. 2). To compare different land covers we chose NDVI pixels that were internally homogeneous regarding land cover. To achieve this, we used a vegetation map derived from a 2004 Landsat 5 TM satellite image. The land cover types selected for this study consisted of: (1) **forests** (mostly pine species resulting from afforestations); (2) **rocky outcrops with thin tussocks** (areas covered by rock and patches of thin tussocks such as *Deyeuxia hieronymi*); (3) ***short grasslands*** (grazing lawns with species such as *Alchemilla pinnata* and *Carex fuscula),* and (4) **thick tussocks** (grasslands dominated by *Poa stuckertii*). For each type of land cover, 4 NDVI pixels of 1km×1km were chosen, trying to minimize internal variability regarding land cover types and maximizing the distance between pixels to reduce spatial dependence.

For each pixel, the HRUs partially or completely contained in it were identified and data derived from the hydrological model were extracted for a each HRU. The variables extracted were precipitation (pp), relative soil saturation (sat) and actual evapotranspiration (ET), and data was converted at the same temporal resolution of NDVI time series (10 daily). To obtain values of these variables for each NDVI pixel, we calculated the fraction of area covered by each HRU in a given NDVI pixel. Each variable was then multiplied by the fraction of the corresponding HRU in the NDVI pixel and then summed across all the HRUs contained in that NDVI pixel. Cross-correlations for several lags were performed using InfoStat software (Di Rienzo et al., 2011) and the maximum coefficient of correlation as well as the lag at which it was recorded were saved for posterior statistical analysis. Maximum correlation coefficients and lags were compared between land cover types and water variables using a non parametric test. We tested the effect of land cover type, water cycle variables and the interaction between them, on both the correlation coefficient and the lags.

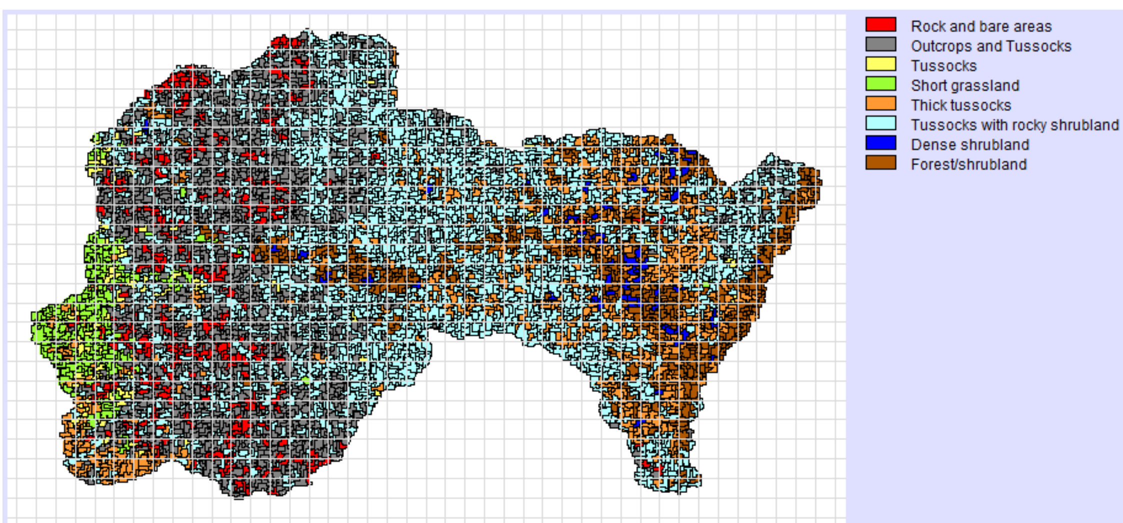


**Figure 2:** HRUs in the San Antonio River Basin. NDVI pixels are shown in light gray and HRUs are colored according to land cover types to show surface composition

## Findings and discussion

The NDVI time series described periodic patterns (within years), depicting changes in vegetation phenological cycles associated with different land-use types (Table 1, Fig. 3). These patterns show seasonal phases: a tendency to a single greenness peak in summer, with limited growth in winter. The maximum values of NDVI were found in forests (0.58) followed by thin tussocks and short grasslands (0.47 and 0.46, respectively), with the lowest values in rocky outcrops with thin tussocks (0.36). NDVI variability was higher in both types of grasslands, thick tussocks and short grasslands, due to higher intra-annual changes of productivity of these vegetation types.

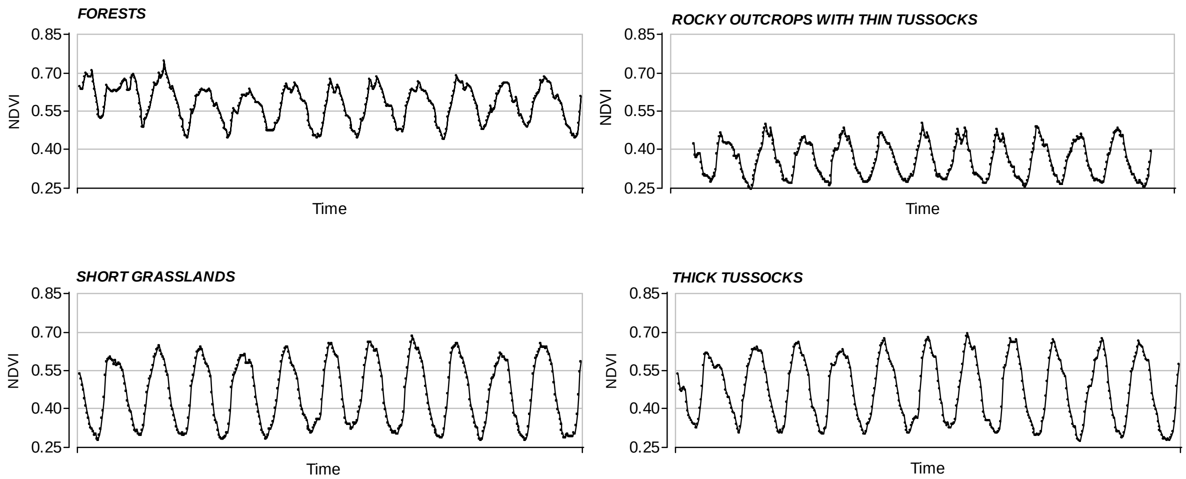


**Figure 3**: Twelve years of smoothed 10 daily composites NDVI values for different land cover types in San Antonio River Basin, Argentina.

**Table 1**: Estimates of NDVI, precipitation (pp), relative soil saturation (sat) and actual evapotraspiration (ET) and their variability as standard deviation in a twelve year period for different land cover types in the San Antonio River Basin.

| LAND COVER TYPE | NDVI | | PP (mm) | | SAT (%) | | ET (mm) | |
|---|---|---|---|---|---|---|---|---|
| | *Mean* | *SD* | *Mean* | *SD* | *Mean* | *SD* | *Mean* | *SD* |
| **Forest** | 0.58 | 0.08 | 21.19 | 25.63 | 41 | 25 | 17.72 | 13.70 |
| **Rocky outcrops & thin tussocks** | 0.36 | 0.07 | 24.04 | 27.96 | 29 | 21 | 12.47 | 10.48 |
| **Short Grasslands** | 0.46 | 0.13 | 17.50 | 25.59 | 35 | 31 | 13.47 | 13.77 |
| **Thick tussocks** | 0.47 | 0.14 | 21.98 | 27.01 | 50 | 29 | 17.63 | 13.02 |

Correlation analysis between the NDVI series and the climate variables (Table 2), calculated by cross-correlation function (CCF), showed positive significant correlations for all variables. The strength of the correlation with NDVI varied significantly between precipitation (pp), relative soil saturation (sat) and actual evapotranspiration (ET) and between land cover types ($p<0.001$), being always higher than 0.5. Actual evapotranspiration was the variable with the highest correlation coefficients for all land cover types, especially for both types grasslands, short grasslands and thin tussocks, with mean values of the maximum correlation coeficients of 0.90 and 0.89, respectively. In forests, although the correlation between NDVI and actual evapotranspiration was the highest, the difference with relative soil water saturation was not as big as in other land cover types (0.71 for NDVI_ET and 0.67 for NDVI_sat). Relative soil water saturation showed higher crosscorrelation coefficients with NDVI than precipitation in short grasslands (0.75 vs. 0.69), thick tussocks (0.74 vs 0.66) and forests (0.67 vs 0.53) but the opposite occurred in rocky areas (0.58 vs. 0.66). Correlations were always lower in forests except for relative soil saturation, which was higher lowest in rocky outcrops with thin tussocks (Fig. 4).

**Table 2**: Maximum correlation coefficients and lags expressed as 10-day periods between NDVI and actual evapotranspiration (NDVI_ET), precipitation (NDVI_pp), and relative soil saturation (NDVI_sat) for different land cover.

| LAND COVER TYPE | NDVI_ET | | | | NDVI_pp | | | | NDVI_sat | | | |
|---|---|---|---|---|---|---|---|---|---|---|---|---|
| | $r_{max}$ | | Lag | | $r_{max}$ | | Lag | | $r_{max}$ | | Lag | |
| | *mean* | *SD* | *mean* | *SD* | *mean* | *SD* | *mean* | *SD* | *mean* | *SD* | *mean* | *SD* |
| **Forests** | 0.71 | 0.03 | 5.25 | 0.96 | 0.53 | 0.01 | 5.75 | 1.50 | 0.67 | 0.01 | 3.00 | 0.00 |
| **Rock & Thin tussocks** | 0.83 | 0.01 | 3.75 | 0.50 | 0.66 | 0.01 | 3.75 | 0.50 | 0.58 | 0.03 | 2.00 | 0.00 |
| **Short Grasslands** | 0.90 | 0.00 | 2.50 | 0.58 | 0.69 | 0.01 | 2.75 | 0.50 | 0.75 | 0.01 | 0.00 | 0.00 |
| **Thick Tussocks** | 0.89 | 0.03 | 2.00 | 0.00 | 0.66 | 0.02 | 3.00 | 0.00 | 0.74 | 0.01 | 0.25 | 0.50 |

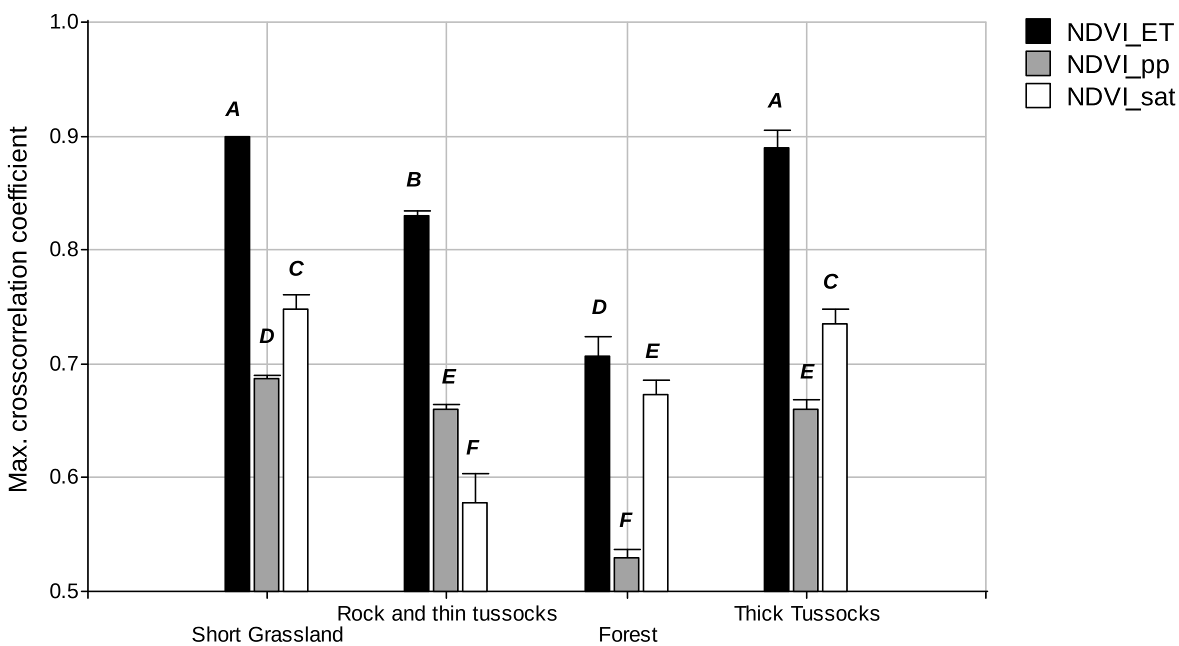


**Figure 4**: Maximum cross-correlation coefficients between NDVI and actual evapotranspiration (ET), precipitation (pp, and relative soil saturation (sat) for different land cover types in San Antonio River Basin, Argentina. Error Bars indicate standard deviation and different letters indicate statistically significant ($p<0.05$) estimates.

Lags at which maximum correlation coefficients were recorded varied significantly between land cover types and between variables, and interaction was significant ($p<0.001$) (Fig. 5). For every land cover type, the response of vegetation to relative soil saturation was the shortest, especially in short grasslands and thin tussocks, where maximum correlation was found for lags of 0 and 0.25, respectively, which means at or almost at the same 10 day period. In forests, the response to soil water content, expresses as percentage of soil saturation, was found at lag 3, which means that forest growth responds to soil saturation between 30 to 40 days later. For all cover types but thick tussocks, vegetation responds to actual evapotranspiration and precipitation with the same delay. However, thick tussocks showed a more delayed response to precipitation than to evapotranspiration. In concordance to what has been found in other studies, forest showed the most delayed response (Weiss *et al.,* 2004) to precipitation and evapotranspiration with lags between 50 to 60 days. Short grasslands respond faster to water availability than rocky areas.

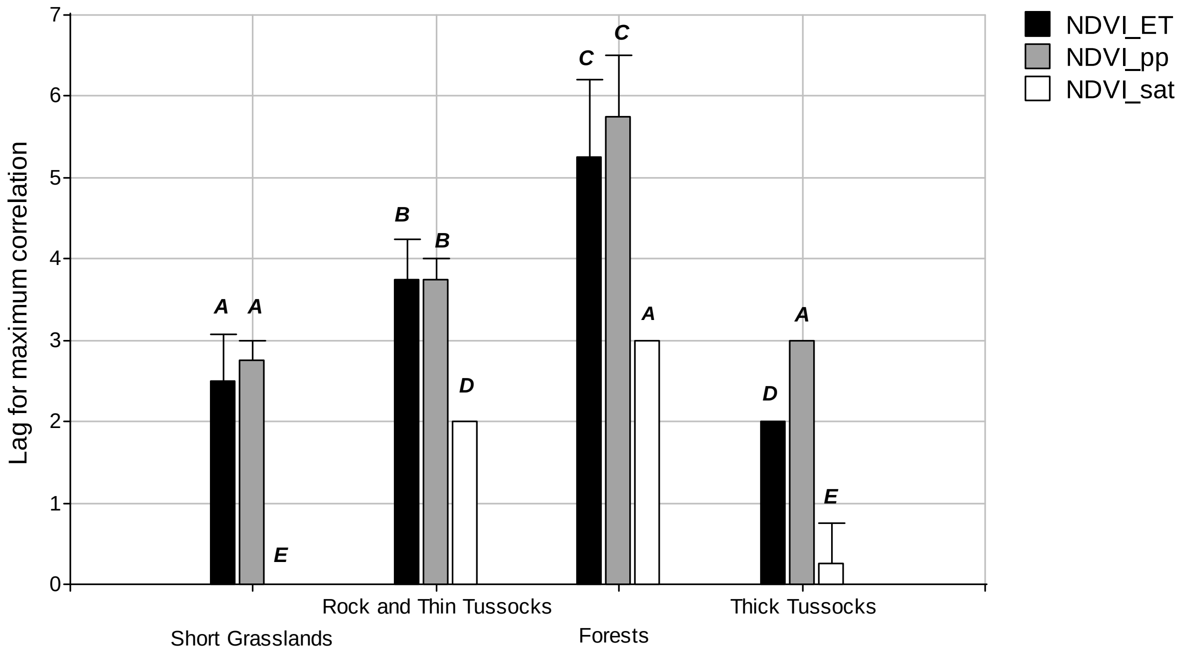


**Figure 5**: Lags at which maximum correlation coefficients between NDVI and actual evapotranspiration (actET), precipitation (pp), and relative soil water saturation (sat) were registered. Error Bars indicate standard deviation and different letters indicate statistically significant ($p<0.05$) estimates.

## Conclusion

The synchrony of the seasonal vegetation pattern with climate differed between the variables considered, depending on the type of land use. Precipitation was always the least correlated variable to vegetation growth, with the exception of rocky areas, which are less vegetated. This areas, associated with poorer soils showed the least correlation with relative soil water saturation. Actual evapotranspiration, always showed the highest correlation with vegetation growth which highlights the importance of temperature as a limiting factor to vegetation growth in the study area. However, synchrony of the vegetation growth with soil water saturation was found to be more direct (less delay), specially in grasslands.

This study shows that hydrological modeling can aid in the study of vegetation response to climate variability, high lightening the importance of taking into account other factors that influence water availability besides precipitation. It allows deepening the understanding of the mechanisms and the interaction between the atmosphere, the topography and the soil, as well as the vegetation. Application of the easily acquired and interpreted NDVI time series data allowed detection of changes in phenological patterns associated with land cover and their modulation by climate. Given its low cost, wide spatial extent and sensitivity to key environmental variables such as those explored here, NDVI time series analysis coupled with hydrological modeling can aid in monitoring programmes, especially in semi-arid environments.

## Acknowledgements

This work was supported by the “GEONETCast for and by Developing Countries” DevCoCast project, that received funding from the EU Seventh Framework Programme for Research and Technological Development (FP7), under Grant Agreement number 211307. First and second authors are Fellows of CONICET and Ph.D. students at the University of Buenos Aires and the National University of Córdoba.

**References**


Cabido, M. (1985) Las comunidades vegetales de la Pampa de Achala, Sierras de Córdoba, Argentina. Documents Phytosociologiques 9:431-443.

Camberlin, P., N. Martiny, N. Philippon and Y. Richard. (2007) Determinants of the interannual relationships between remote sensed photosynthetic activity and rainfall in tropical Africa, Remote Sensing of Environment, 106:199- 216.

Chamaille-Jammes, S., H. Fritz and F. Murindagomo. (2006) Spatial patterns of the NDVI-rainfall relationship at the seasonal and interannual time scales in an African savanna. Int. J. Remote Sensing, 27(23-24): 5185-5200.

Cingolani, A. M., D. Renison, M. Zac, y M. Cabido. (2004) Mapping vegetation in a heterogeneous mountain rangeland using Landsat data: an alternative method to define and classify land-cover units. Remote Sensing of Environment 92(1):84-97.

Eerens H. (2010) *Manual of GLIMPSE, Global Image Processing Software.* VITO TAP, Mol, Belgium.

Flügel, W-A. (1995) Delineating Hydrological Response Units (HRU's) by GIS analysis for regional hydrological modelling using PRMS/MMS in the drainage basin of the River Bröl, Germany. - Hydrological Processes, 9:423-436.

Jobbágy, E.G., O.E. Sala, and J.M. Paruelo. (2002) Patterns and controls of primary production in the patagonian steppe: a remote sensing approach. Ecology 83:307–319.

Kogan F.N. (2000) Satellite-observed sensitivity of world land ecosystems to El Niño/La Niña. Remote Sensing of Environment, 74:445-462.

Kralisch, S. and Krause, P. (2006). JAMS – A Framework for Natural Resource Model Development and Application. In Voinov, A., Jakeman, A., and Rizzoli, A., editors, Proceedings of the iEMSs Third Biannual Meeting ”Summit on Environmental Modelling and Software”, Burlington, USA.

Krause, P. (2002) Quantifying the impact of land use changes on the water balance of large catchments using the J2000 model; Physics and Chemistry of the Earth, 27:663-673.

Krause, P. and Hanisch, S. (2009) Simulation and analysis of the impact of projected climate change on the spatially distributed waterbalance in Thuringia, Germany, Advances in Geosciences, 21:33–48.

Lewis JE, Rowland J, Nadeau A (1998) Estimating maize production in Kenya using NDVI: some statistical considerations. International Journal of Remote Sensing, 19:2609–2617.

Li Z, Kafatos M. (2000) Interannual variability of vegetation in the United States and its relation to El Niño/Southern Oscillation. Remote Sensing of Environment, 71:239-247.

Ludeke, M.K.B., Ramge, P.H., Kohlmaier, G.H., (1996) The use of satellite NDVI data for the validation of global vegetation phenology models: application to the Frankfurt Biosphere Model. Ecol. Model. 91:255–270.

Nosetto M.D, Jobbágy E.G, Brizuela A.B, Jackson R.B. (2011) The hydrologic consequences of land cover change in central Argentina. Agricultural, Ecosystems and Environment. In press.

Samani , Z. (2000) Estimating Solar Radiation and Evapotranspiration Using Minimum Climatological Data . Journal of Irrigation and Drainage Engineering 126(4):265-267.

Seaquist, J.W., Olson, L., Ardo, J. (2003) A remote sensing-based production model for grassland biomes. Ecol. Model. 169:131–155.

Swets DL, Reed BC, Rowland JD, Marko SE (1999) A weighted least-squares approach to temporal NDVI smoothing. Proceedings of the 1999 ASPRS Annual Conference, Portland, Oregon, 526-536.

Tucker C.J. (1979) Red and photographic infrared linear combinations for monitoring vegetation. Remote Sensing of Environments, 8:127-150.

Viglizzo E.F, Frank F.C, Carreño L.V, Jobbágy E.G, Pereyra H, Clatt J, Pincén D, and Riccard MF. (2010) Ecological and environmental footprint of 50 years of agricultural expansion in Argentina. Global Change Biology. doi: 10.1111/j.1365-2486.2010.02293.x.

Walther G.R., Post E., Convey P., Menzel A., Parmesan C., Beebee T.J.C., Fromentin J.M., Hoegh-Guldberg O. & Bairlein F. (2002) Ecological responses to recent climate change. Nature 416:389–395.

Weiss, J.L., Gutzler, D.S., Coonrod, J.E.A. and Dahm, C.N., 2004, Seasonal and interannual relationships between vegetation and climate in central New Mexico, USA. Journal of Arid Environments 57: 507–534.